View metadata, citation and similar papers at core.ac.uk
brought to you by CORE
provided by The University of Utah: J. Willard Marriott Digital Library

Quantitative two-dimensional dopant profile measurement and inverse modeling by scanning capacitance microscopy

Y. Huang and C. C. Williams
Department of Physics, University of Utah, Salt Lake City, Utah 84112

J. Slinkman
IBM Microelectronics, Essex Junction, Vermont 05452

(Received 19 August 1994; accepted for publication 7 November 1994)

Quantitative dopant profile measurements are performed on a nanometer scale by scanning capacitance microscopy (SCM). An atomic force microscope is used to position a nanometer scale tip at a semiconductor surface, and local capacitance change is measured as a function of sample bias. A new feedback method has been demonstrated in which the magnitude of the ac bias voltage applied to the sample is adjusted to maintain a constant capacitance change as the tip is scanned across the sample surface. A quasi-1D model is used to extract dopant density profiles from the SCM measurements. The inverted SCM dopant profiles are compared with profiles obtained by process simulation and secondary ion mass spectroscopy measurement. Good agreement was found between the SCM measured profile and the lateral profile predicted by SUPREM 4 over the concentration range from 10^{17} to 10^{20} cm^{-3}. © *1995 American Institute of Physics.*

With the shrinkage of semiconductor devices to the submicron level, a great need exists for direct quantitative two dimensional (2D) dopant profile measurement on a nanometer scale. First, direct measurement of 2D dopant profile provides a means for improving very large scale integrated (VLSI) process and electrical device simulators. Direct 2D profile measurements are needed to accurately calibrate and verify models built into these simulators. Additionally, direct 2D measurements can also give rapid feedback to improve control of manufacturing processes and decrease process development time.

There are many 1D dopant profiling techniques presently available, such as secondary ion mass spectroscopy (SIMS), spreading resistance, junction staining (TEM), and anodic sectioning.[1] These standard techniques do not provide quantitative 2D dopant profile information. The advent of the scanning tunneling microscope (STM) and the more recent scanning probe microscopies (SPMs) have provided a new direction for direct device characterization on a nanometer scale.[2–9] The scanning capacitance microscope (SCM), in particular, has shown great potential for direct measurement of 2D dopant profile with nanometer scale spatial resolution.[10–12] To date, SCM measurements have largely been qualitative in nature due to the fact that a complex analysis is required to quantitatively invert local SCM measurements to dopant profile.[11,12] Here we report on the development of a new SCM approach for semiconductor characterization which simplifies the inversion of SCM data to dopant profile.

The SCM dopant profiling approach is based upon the general concepts used in 1D capacitance-voltage (C-V) profiling.[13] In particular, the SCM approach is based upon the measurement of carrier density, rather than impurity concentration (dopant density) directly. It has been shown, however, that when the dopant density varies moderately over a scale comparable to the Debye length (Debye length is 13 nm) at a concentration of 10^{17} cm^{-3} and 0.4 nm at 10^{20} cm^{-3}), the carrier density is a reasonably good measure of the activated dopant density.[13] Since in the work described here the profiles are not abrupt on the scale of a Debye length (for concentrations above 10^{17} cm^{-3}), we will refer to the SCM measured profiles as dopant density profiles.

Our instrument is a combination of an atomic force microscope (AFM) and a SCM.[12] The block diagram of our setup is shown in Fig. 1. A tungsten tip is brought to the surface of a silicon MOS structure. A contact mode AFM is used to position and scan the tip over the surface of the sample. A high sensitivity capacitance sensor (operating at 915 MHz) is connected to the tip to measure the capacitance between the tip and sample. The tip is grounded at low frequencies with an inductor and a 4 kHz ac bias voltage is applied to the sample. The tip/sample capacitance change associated with the ac bias voltage (due to semiconductor depletion) is measured by the capacitance sensor and detected by lock-in amplifier. The detected signal is compared to a reference voltage and sent to a feedback controller. The feedback controller adjusts the magnitude of the ac bias voltage applied to the sample [via a voltage controlled oscillator

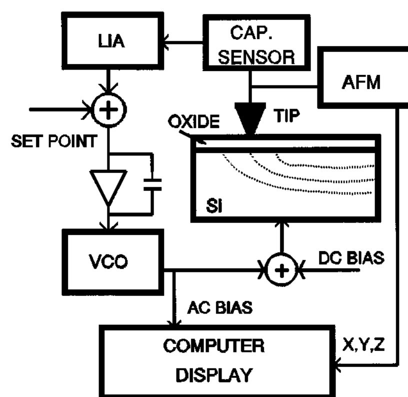

FIG. 1. Block diagram of the scanning capacitance microscope and new feedback system.

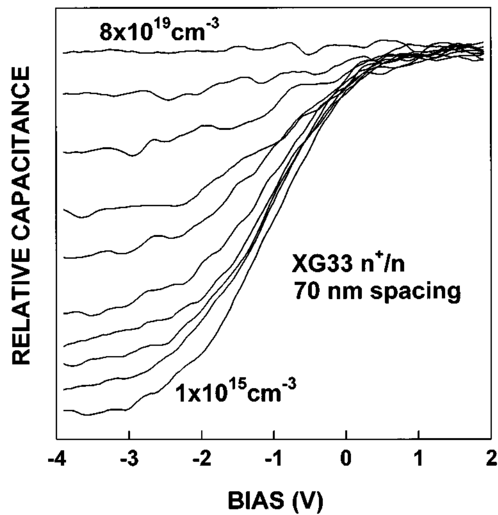

FIG. 2. A set of C-V curves measured at ten different locations across the implantation edge with 70 nm spacing. Only the curves with highest and lowest dopant density are identified by dopant density numbers.

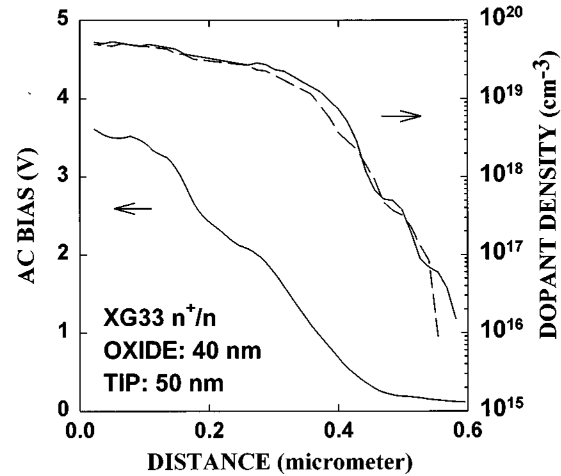

FIG. 3. The feedback controlled ac bias voltage measured by SCM as the tip moves across the implantation edge (left-hand side). Two inverted SCM dopant profile curves measured with the same probe tip shown as a measure of repeatability (right-hand side).

(VCO)] so as to keep a constant ac capacitance change (depletion) as the tip is scanned over regions of varying dopant density. The feedback controlled magnitude of the ac bias voltage is recorded by computer along with the AFM topography signal as the probe is scanned across the sample. The SCM measurements can thus be directly correlated with the topographic surface profile.

The probe tips are fabricated by electrochemically etching 50 μm tungsten wires in 2 M NaOH solution. A 20 nm radius of curvature can be achieved by this method. The samples were prepared by window-implanting (resist mask) n-type silicon wafers (6×10^{14} cm^{-3}) with phosphorus ions at 80 keV through a 22 nm oxide. The peak concentration at the surface in the implanted region was measured by SIMS to be 8×10^{19} cm^{-3} (n type). The oxide in the unmasked region was then chemically removed and the resist mask was then stripped. The wafers were reoxidized (40 nm oxide) in a wet ambient at 900 °C for 20 min. An 8 nm step in the oxide was measured near the original location of the mask edge by AFM. This edge step was used to determine approximately the lateral position of the implant edge.

Figure 2 shows ten full C-V curves measured with the SCM probe at 70 nm spacings near the implantation edge using a previously described boxcar averaging technique.[12] The dopant density corresponding to the lowest and the highest C-V curve is approximately 1×10^{15} and 8×10^{19} cm^{-3} respectively. Note that the shape and size of the curves monotonically change with dopant density over this dopant density range. While it is difficult to see on this scale any capacitance change between depletion and accumulation at the highest concentration, this capacitance change can be measured easily by a lock-in amplifier.

This same sample was then imaged using the new constant capacitance change feedback mode. The feedback loop set point was adjusted so that a very small capacitance change at each position was maintained by the feedback loop. The left curve shown in Fig. 3 represents the feedback controlled magnitude of the ac bias as the tip was scanned across the implantation edge. The change in slope of the ac bias voltage curve around 0.2 μm is systematic and is due to the small surface step in the oxide.

Under the new feedback control, the depletion depth beneath the tip should remain approximately the same for regions of different dopant density. If the depletion depth chosen by the set point is small compared to the tip size and oxide thickness, a quasi-1D model can be used to invert the SCM data to dopant profile. Below is a brief description of the quasi-1D model that has been developed for inversion of the SCM data. It will be described in detail elsewhere.[14] The tip is represented by a conducting sphere in contact with an oxide on a conducting plane. The whole surface plane of the sample is divided into narrow annuli around the contact point between the tip and oxide. For each annular radius, the effective insulator capacitance (oxide and air) is calculated by the method of images assuming no depletion. Once the effective gap capacitances are known for each radius, the depletion depth can be calculated for a given tip bias voltage, assuming that the depletion depth is small. The depletion capacitance in the silicon is calculated for each annular region using a simple 1D band bending model.[13] The total capacitance for each annular region is obtained by adding, in series, the effective insulator capacitance and the silicon depletion capacitance for that annular region at a given tip/sample bias voltage. The total tip/sample capacitance is obtained by integrating the capacitance contribution of each of these annular regions. The tip/sample capacitance can thus be obtained as a function of tip bias, tip radius, dielectric thickness, dopant density, and annular radius.

Our calculations indicate that the total capacitance between tip and sample converges very slowly as the integration of the annular capacitance contributions is performed. This is expected, since the stray capacitance is much larger than that due to fields directly below the tip. In our SCM measurements, however, only the capacitance change due to

depletion under the applied ac bias is measured. Our calculations show that the capacitance change converges with integrated radius much faster than the total capacitance itself. Furthermore, the capacitance change at the higher dopant densities is dominated by depletion which occurs in the silicon within 1 tip radius of the contact point. This indicates that the expected spatial resolution is just equal to the tip diameter. Due to the high operating frequency of the capacitance sensor, the spreading resistance in the Si substrate (in series with the tip/sample capacitance) can potentially influence the measured capacitance. However, for small tip radii (sub-100 nm) and for dopant densities of 10^{17} cm^{-3} or greater, these spreading resistance effects can be shown to be negligible.

Only relative dopant profiles can be performed by the SCM method without the use of dopant density standards. A reference point at which the dopant density is known by an independent means is needed to find the absolute dopant profile. Here we use the highest dopant density (predicted by SUPREM 4[15]) as the reference point to invert the magnitude of the ac bias to absolute dopant profile. All values of the SCM profile are determined by comparison to this dopant density. A numerical inversion algorithm was written based upon our quasi-1D model to invert the SCM feedback data (magnitude of the ac bias versus lateral position) to dopant density profile. The measured values for oxide thickness (40 nm) and tip radius (50 nm) are used in the inversion calculations. Since the work function difference between tip and sample is not well known, we tried the inversion with several different work function difference values. We found that the best fit resulted if the tungsten Fermi level was placed 0.15 eV below the midgap of silicon. However, we also found that the inversion depends only weakly upon the work function difference for dopant densities above 10^{17} cm^{-3}.

The curves on the right-hand side of Fig. 3 display the repeatability of the inverted SCM dopant profile measurements. The same tip was used two times at the same location. The two curves are very similar except in the lower dopant density region where the quasi-1D inversion model becomes hypersensitive to small variations in ac bias. Figure 4 shows the average of the SCM lateral profile curves shown in Fig. 3 compared with a lateral simulation profile (SUPREM 4) and a vertical SIMS profile for reference. It is well known that vertical and lateral dopant profiles are generally different. Above a dopant density of approximately 10^{17} cm^{-3}, the SCM measured profile fits the lateral simulation profile very well. The fit is particularly remarkable since all of the SCM profile has been obtained by comparing the SCM response at the highest dopant density with every other point. The use of dopant standards should significantly improve the overall accuracy.

Below 10^{17} cm^{-3}, the error between SCM and simulated profiles becomes larger. In fact, the inversion of the SCM data below 10^{16} cm^{-3} diverges quite strongly from the simulated profile. At these dopant densities, the Debye length becomes comparable to the tip size, and the quasi-1D approximation breaks down. For characterization of current VLSI structures, the important dopant density range is from 10^{17} to 10^{20} cm^{-3}. The SCM appears to perform well in this range. Improvement in the inversion model may further extend the range over which the SCM can provide accurate dopant profiling.

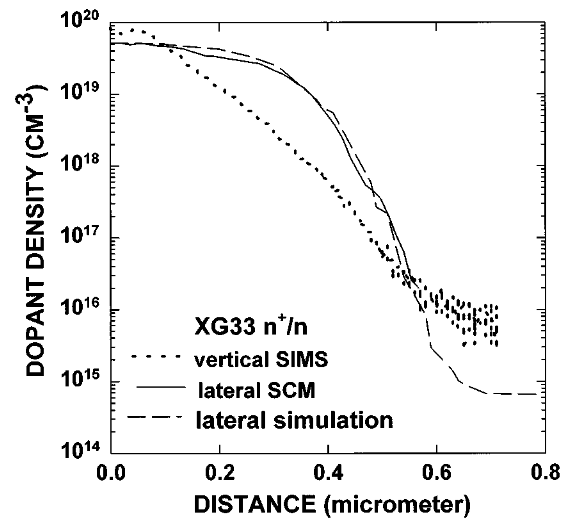

FIG. 4. Comparison of the SCM measured profile with a SUPREM IV profile near the implantation edge. The vertical SIMS profile is also shown for reference.

In summary, we have performed direct dopant profile measurements on implanted silicon wafers by a novel SCM technique. A new constant capacitance change feedback method is used to simplify the inversion of the SCM data. A quasi-1D model has been generated to invert the experimental SCM data to dopant density. The inverted SCM profile has been compared with SIMS and simulation results. The SCM measured profile is in good agreement with lateral simulation profiles over a dopant density range of 10^{17}–10^{20} cm^{-3}.

The authors would like to thank Y. Leng, J-K. Leong, A. DiCarlo, and R. Davis for their general contribution to this work. The work was supported by the Semiconductor Research Corporation.

[1] R. Subrahmanyan, J. Vac. Sci. Technol. B **10**, 358 (1992).
[2] P. Muralt, H. Meier, D. W. Pohl, and H. W. M. Salemink, Appl. Phys. Lett. **50**, 1352 (1987).
[3] S. Hosaka, S. Hosoki, K. Takata, K. Horiuchi, and N. Natsuaki, Appl. Phys. Lett. **53**, 487 (1988).
[4] Y. Martin, D. W. Abraham, and H. K. Wickramasinghe, Appl. Phys. Lett. **52**, 1103 (1988).
[5] D. W. Abraham, C. C. Williams, J. Slinkman, and H. K. Wickramasinghe, J. Vac. Sci. Technol. B **9**, 703 (1991).
[6] M. B. Johnson and J.-M. Halbout, J. Vac. Sci. Technol. B **10**, 508 (1992).
[7] S. Kordic, E. J. vanLoenen, and A. J. Walker, J. Vac. Sci. Technol. B **10**, 508 (1992).
[8] M. B. Johnson, H. P. Meier, and H. W. M. Salemink, Appl. Phys. Lett. **63**, 3636 (1993).
[9] C. Shafai, D. J. Thomson, M. Simard-Normandin, G. Matiussi, and J. Scanlon, Appl. Phys. Lett. **64**, 342 (1994).
[10] C. C. Williams, J Slinkman, W. P. Hough, and H. K. Wickramasinghe, Appl. Phys. Lett. **55**, 1662 (1989).
[11] K. S. Mak and C. C. Williams, Proc. SPIE **1556**, 90 (19920.
[12] Y. Huang and C. C. Williams, J. Vac. Sci. Technol. B **12**, 369 (1994).
[13] E. H. Nicollian and J. R. Brews, *MOS Physics and Technology* (Wiley, New York, 1982).
[14] Y. Huang and C. C. Williams (unpublished).
[15] SUPREM IV, version 6, Technology Modeling Associates, Palo Alto, CA.